



Microwave- Assisted Synthesis of Nano/Micronized Zeolites from Natural Sources: Evaluation of Hydrogen Storage Capacities



Hanan F. Youssef ^{a*}, Nahla Ismail^{b*}

^aInorganic Chemical Industries, ^bPhysical Chemistry Department, National Research Centre, El-Behouth St., Dokki, Giza, 12622, Egypt

Abstract

This is a comparative study to investigate the hydrogen Storage ability of three zeolites; Zeolite-A, Faujasite-NaX and Analcime, prepared via microwave technique from refined kaolin. The paper addresses the effects of crystallite size, Si/Al, pore diameter and specific surface area on the hydrogen uptake capacity. X-Ray Fluorescence is used for rock chemical analysis, X-ray Diffraction for zeolite mineralogy, Scanning Electron Microscopy and Transmission Electron Microscopy for microstructure. Whereas, Electron Dispersion Analysis monitored the chemical microanalysis. Storing hydrogen is processed via Pressure, Composition and Temperature, using AMC PCI-HP 1200 equipment, meanwhile, BEL Sorb Max device (BEL JAPAN. INC) is used for specific surface area.

Result indicates that, decreasing crystallite size has positive effects on both total pore volume and specific surface area, with a net result of higher hydrogen gravimetric capacities for all structures. At 77K and 22 bar, nano- Faujasite presents the highest hydrogen uptake of 2.25 wt%, whereas, nano Analcime hosts the least amounts of hydrogen of 0.74 wt%. Despite of the effect of zeolite particle size reduction on the surface area enlargement and high adsorption capacity, the limiting factor in hydrogen uptake into zeolite porous vicinities is the diameter of the pores and the blocking effects of their channels.

Key words: Hydrogen storage; Microwave synthesis; Nano-zeolites; natural resource

*Corresponding author e-mail: hanan_eltantawy@yahoo.com; nahlaismail24@yahoo.com.

Receive Date: 29 December 2019, Revise Date: 24 January 2020, Accept Date: 16 February 2020

DOI: 10.21608/EJCHEM.2020.21421.2290

©2020 National Information and Documentation Center (NIDOC)

1. Introduction

While hydrogen production and conversion are already technologically feasible, its delivery and storage are facing serious challenges that hindering its widespread application as a promising clean form of energy. The main obstacle is to develop a safe, reliable, compact, recyclable and cost-effective storing technology. Hydrogen can be stored via: 1) physical storage of compressed gas in high pressures tanks (up to 10,000 pounds per square inch); 2) physical storage of cryogenic liquid (cooled to -253°C) in insulated tanks; and 3) storage within the structures or on the surfaces of certain advanced microporous materials. Actually, the current conventional systems have serious limitations in transportation in respect to safety, energy loss on mobility and vehicle overloads. Furthermore, the previous used systems can be seemingly affordable by chemical and refining industries, but it remains costly inconvenient for many other energy applications.

Solid state storage is addressed as the proper alternative for the previous H_2 storing (HS) problems, where hydrogen can be combined with solids either physically or chemically and be released whenever needed by any technique such as thermal means, hydrolysis, etc. For a material to be considered as a relevant storing media, it has to meet the revised proposed target of US Department of Energy (DOE) and the Freedom CAR agreement for 2015 for on-board hydrogen storage specifications of 5.5 wt% and 40 g/L (5-13 Kg) at 233-538K and 3-100 bars. This facilitates a light car to travel 500 Kms without need to refuel [1-5]. In addition, any proposed media should suitably meet an appropriate cost of 4\$/KWh and be safe in accidents [6-7].

Porous solids are highly considered as relevant media for HS and can accommodate hydrogen

through adsorption or absorption onto and/or within their high surface areas [8-9]. In adsorption, molecules (H_2) of hydrogen can be attached to the surfaces of a material by the weak van der Waals interaction, i.e. with a small enthalpy of adsorption (ΔH_a) between 4-10 KJ/mol, which reflects the ease of hydrogen recovery and reversibility. This process is aided by the capillary condensation in the tiny channels and pores of the material. Meanwhile, in absorption, hydrogen molecules dissociate into hydrogen atoms that are incorporated into the solid lattice frameworks. The later method is promising for storing larger quantities of hydrogen in smaller volumes at mild pressure and at temperatures close to room temperature. Also, hydrogen can be stored in the layered materials, MPS_3 , where, M is transition metal (Fe, Mn, V, etc.) [10-11]. Finally, hydrogen can be strongly bound within molecular structures, as chemical compounds containing hydrogen atoms as in ammonia borane, hydrides, amides, composite materials, metal-organic frameworks, organic molecules, etc. [12-14]. Zeolites, carbon materials, polymers, and metal-organic frameworks are among the highly porous materials considered for storing different gases containing hydrogen [15-18]. Although, some metals (hydrides) indicated high storage capacities for hydrogen, their large binding energies, slow kinetics and high temperature of regeneration are limiting their on-board application. In the same context, the reversibility and fast kinetics of carbon structures (active forms, nanotubes and other forms) seemed to be the right choice for the needed storing material. However, being of low storing capabilities at ambient conditions, implying different uptake capacities when prepared with different routes, and the necessity of cryogenic temperature for attaining high H_2 storage, greatly hindered their practical applications [19].

Zeolites are microporous inorganic solids with an effective pore size range of about 0.3 – 1.0 nm and a vast specific surface area of more than 900 m²/g. Their frameworks are highly considered for physisorbed molecular hydrogen storage since their pore dimensions are less than 0.7 nm, which is close to the single hydrogen molecule size. Compared to the gas phase, microporous zeolites can imply significant increase in the HS density at any given temperature and pressure due to the overlapping of the adsorption potentials of the opposing pore walls. Generally, most of zeolite pores are smaller than the kinetic size of a hydrogen molecule in ambient temperature and can only be enclosed within pores under elevated temperatures and pressures. Practically, by reducing the temperature, the hydrogen is trapped into zeolite framework cavities and channels, but can be released again when the temperature is re-elevated [20-21].

Many types of zeolites were naturally originated and number of them are also synthetically prepared, some of which are to be of special interest in this study. Analcime (analcite) mineral occurs naturally accompanying other zeolites in many basic igneous rocks such as basalt, and also in prehnite, calcite and zeolites as the cavity and vesicle filling [22]. It has NaAl (Si₂O₆) · H₂O empirical formula and usually crystallizes in the cubic, orthorhombic and tetragonal systems. Its structure forms of chains of single connected 4-membered rings and likely configures in the characteristic trapezohedral form [23-24]. Whereas, Faujasite–Na is an isometric synthetic zeolite which is the analogue of the natural Faujasite mineral with a structure containing chains of 6-membered rings and (Na₂, Ca, Mg)_{3.5}[Al₇Si₁₇O₄₈] · 32H₂O general formula. Depending on the silica-to-alumina ratio of their framework, synthetic faujasites are divided into X and Y types. In X-zeolite form, the Si/Al ratio is between 2 and 3, while in Y version it is 3 or higher [25]. Finally,

Zeolite-A is the first manufactured zeolite, which introduced 1949 with no natural counterpart. It is one of the synthetic molecular sieves that covers various applications such as in detergents and desiccants, adsorption, separation, catalysis, and ion exchange [26].

The nanoporous framework structure of aluminosilicate zeolites was considered as a safe solid carrier for hydrogen energy storage, Table1 summarizes some volumetric hydrogen storing capacities of some members of this group of minerals.

Table 1: Hydrogen storage in some aluminosilicate zeolite structures

Zeolite type	Hydrogen uptake (wt%)	Loading conditions	Reference Number
Zeolite-NaX	0.84	75K,1bar	[27]
Zeolite-A (Ca)	0.97 0.79		
Zeolite-A(Na)			[28]
Zeolite-NaX	0.9	77K,760mmHg	
Zeolite-NaX	0.21	100K,6MPa	[29]
Zeolite-NaX	0.6	77K, 0.6 bar	[30]
Zeolite-NaY	0.17		[31]
Zeolite-A(Na)	1.2	RT, 700 bar	
Zeolite-CaX	2.19	77K,15 bar	[32]
Zeolite-Li X	1.5	77K, 1 atm.	[33]
	0.5	298K, 10 MPa	[34]
Zeolite-NaX	0.7	77K, 1 bar	

Although zeolites implied limited theoretical value for its possible maximum hydrogen storage capacity of 2.86% [34], arguments against their lower contribution led in all cases to the feasibility of continuous investigation of their structures as being a model system for the hydrogen and microporous materials interaction [36-37]. As a porous material, zeolites show a complete reversibility of the adsorption process with rapid kinetics [38-39], in contrast to metal and complex hydrides-based hydrogen adsorption process. In addition, no crystallographic phase changes are induced through the physical adsorption of hydrogen and the zeolites indicated high stability in repeated hydrogen cycling [40]. In addition, Zeolites are non-flammable either in

air or in H₂, chemically tunable to trap hydrogen at room temperature and can feasibly be prepared in large industrial scale with high quality and low cost.

In the present work, three zeolites with different Si/Al ratios, pore diameters, crystallite sizes and specific surface areas namely; Zeolite-A (ZA), Faujasite-NaX (ZX) and Analcime (ANA) were hydrothermally prepared in both nano and micronized forms, using microwave technique, from refined kaolin and assessed for storing hydrogen. The performance of all produced powders for storing hydrogen, was evaluated in relation to their corresponding Si/Al composition, crystallite sizes, surface areas and pore diameters.

2. EXPERIMENTAL

Refined kaolin, supplied by Middle East Mining Company (MEMCO), was used as the starting material (to avoid interfering phases on processing), its chemical composition (in wt%) contained 53.25 SiO₂, 42.94 Al₂O₃, 0.41 Fe₂O₃, 1.62 TiO₂ and some other minor constituents of MgO, CaO, K₂O. Sodium hydroxide pellets (NaOH) of analysed ACS reagent with the composition of 98.6% NaOH+ 0.4% chloride (Sigma-Aldrich) was applied. Ludox 40 was the source of additional SiO₂ for adjusting the kaolin composition to meet the targeted zeolite formula. The batch composition of the starting rock and the corresponding gel modification to the targeted zeolites are given in Table 2.

Table 2: Batch composition of the starting gel of all zeolites.

Materials (Ratios)	Zeolites batch Composition (Ratio)		
	Zeolite- A(ZA)	Analcime (AN)	Faujasite- Na (ZX)
SiO ₂ /Al ₂ O ₃	1-1.2	4-8	4-8
NaOH	2.5-4	2-4	4-6
Molarity			
H ₂ O/SiO ₂	100-150	100-200	100-200

2.a. Preparation of zeolite slurry from kaolin

The starting kaolin was calcined at 700 °C for 2h to be converted into metakaolinite (amorphous form of kaolin). Based on the equal ratios of Si and Al in both kaolinite and zeolite-A (Si/Al~1), the latter is directly prepared from calcined kaolin without any modification, following the method of “Youssef et.al., 2008” [41], where 10 g of thermally treated rock powder was reacted with 100 ml of 3.0 molar caustic soda and stirred at 700 rpm for 30 min. In case of Faujasite-NaX and analcime, Si/Al ratios of the precursor powders are adjusted to meet the targeted zeolite. In a typical method, two separate polypropylene beakers containing 50 ml of 3.0 M NaOH were placed on vigorous stirring; to the first one, 40 ml of Ludox was gradually added and stirred for 30 min, whereas, 10 g of the calcined kaolin were added to the second beaker on stirring for another 30 min. The two solutions were then mixed and the final slurry was additionally stirred overnight.

2.b. Microwave hydrothermal treatments (M-H)

The freshly prepared gel (slurry) is heated for different durations ranging from 1 to 4h for obtaining the micro and nano species of zeolites at 150-160°C for analcime, 110°C for faujasite-NaX and for 80 °C for zeolite-A [41-43]. Typically, an amount of 25 ml of the previously prepared slurry was batched and heated in the 100 ml capacity Xpress vessels of microwave digestive system (Mars 5, Model XP-1500, CEM Corp., Matthews, NC). The system operates at a frequency of 2.45 GHz and can operate at 1–100% of 1600W power. After heat treatment, the prepared powders were collected, washed several times with distilled water and then dried at 100 °C overnight in an electric oven. The clean dry products are then being ready for different characterization.

2.c. Characterization techniques

In the present study, the chemical analysis of the starting Kaolin was obtained by X-ray fluorescence using XRF instrument model AXIOS, WD-XRF Sequential Spectrometer (Panalytical, 2005). Meanwhile, the mineralogical constituents of prepared zeolites were investigated by X-ray diffraction method, using Bruker D8 Advance with secondary monochromatic beam CuK radiation at $Kv = 40$ and $mA = 40$. Microstructures of the prepared micro-materials were scanned using SEM model Quanta 250 FEG (Field Emission Gun) attached with EDX Unit (Energy Dispersive X-ray Analyses), with accelerating voltage 30 K.V., magnification 14x up to 1000000 and resolution for Gun.1n). FEI Company, Netherlands. The nanostructures of the phases were monitored using TEM, model JEOL, JEM-2100 Electron Microscope, High Resolution TEM, power 200 KV, Resolution 1.4 Å, Made in Japan.

The specific surface area, pore and particle size distribution of the prepared zeolites were determined from nitrogen adsorption–desorption isotherms were measured with a high-speed gas sorption analyzer (NOVA 2000 series, chromatic, UK) at 77 K. Before measurements, the samples were out-gassed at 150 °C in vacuum for 6 h. The Barrett–Emmett–Teller (BET) method was utilized to calculate the specific surface areas. The pore-size distributions were derived from NLDFT method. The total pore volume was estimated from the amount adsorbed at a maximum relative pressure.

The determination of hydrogen content was carried out by the measurement of pressure-composition isotherms (PCI) by a volumetric method using an AMC PCI-HP 1200 equipment. 0.5 g of the sample was placed in the test chamber. Then the pressure was evacuated to 0.01 bar and heated till 200 °C/2h for degassing. Then cooled to 77K using a cryostat and the hydrogen pressure was applied gradually till 20 bar. The hydrogen absorption is recorded automatically from the

programmed device and the Pressure-Composition Isothermal (PCI) plots were traced under the above mentioned conditions. Temperature was controlled with a precision of -0.1 °C. The accuracy of hydrogen content measurements was ± 0.04 wt%.

3. RESULTS AND DISCUSSIONS

In the current study, the nano and micro forms of zeolite types will, afterwards, be assigned as N and M, respectively. The following abbreviations will be concerned; N-ZA & M-ZA, N-ZX & M-ZX, and finally N-ANA & M-ANA for the nano and micronized zeolite types as follows; zeolite-A, faujasite-NaX, and analcime, respectively.

3.a. XRD Results

Figures 1-3 present the X-ray diffraction patterns for the prepared zeolites in their nano and micro-sizes of Analcime, Faujasite-NaX and, Zeolite-A, respectively. In all figures, the XRD for the parent kaolin and its corresponding amorphous form, metakaolinite, were set as the base line in the XRD patterns of all produced zeolites for comparison.

Figure 1 shows the XRD patterns of the formed powders prepared under different microwave conditions. Analcime, also called analcite (ANA), phase with the orthorhombic(pseudocubic) form and $Na_{16.8} Al_{15.84} Si_{32.16} O_{95} \cdot 16 H_2O$ chemical formula was crystallized from the precursor gel at temperatures of 150°C for 4h (M-ANA) and 160°C/1h (N-ANA), respectively. The determined XRD peak intensities and positions of micro and nano analcime powders were completely matching with those in the reference PDF card #83-1736.

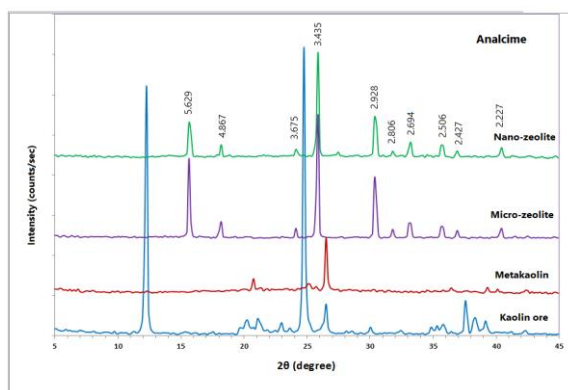


Figure 1: Analcime zeolite prepared at 150°C for 4h (micro) and 160°C for 1h (nano) under M-H.

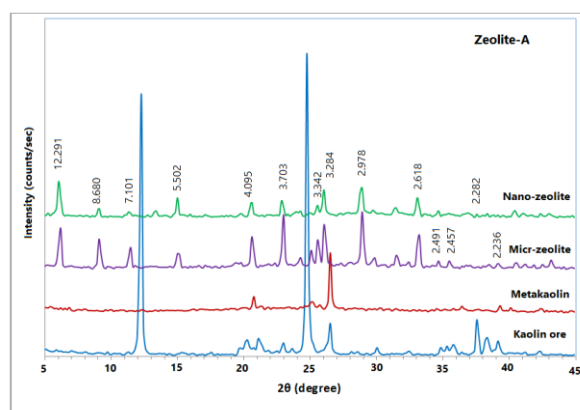


Figure 3: Zeolite-A prepared at 80 °C /4h (Micro) and 80 °C /1h (Nano) under M-H conditions.

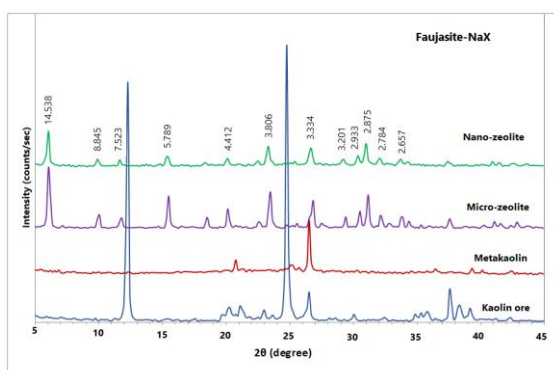


Figure 2: Faujasite-NaX powders prepared at 110°C for 4h (Mico) and for 1h (Nano) under M-H conditions.

Figure 2 illustrates the XRD data for the faujasite-NaX, also called zeolite-X (ZX), samples prepared under conditions of 110 °C/ 1h (N-ZX) and 4h (M-ZX), respectively. The d -spacing of the formed powders was in good consistent with cubic Faujasite-NaX with the typical formula of $\text{Na}_2 \text{Al}_2 \text{Si}_4 \text{O}_{12} \cdot 8 \text{H}_2\text{O}$ and PDF # 39-1380 reference card.

Figure 3 depicts the X-ray diffraction profile for zeolitic products resulted from the reaction of metakaolinite with 3.0M NaOH and heated at 80°C/4h (M-ZA) and for /1h (NZA) under M-H conditions, respectively. The peak intensities and positions of both micro and nano powders have been accertained the crystallization identity of the Linde Type A zeolite, also called zeolite-A or 4A zeolite (ZA), with the same chemical formula of $\text{Na}_{12}\text{Al}_{12}\text{Si}_{12}\text{O}_{48} \cdot 27\text{H}_2\text{O}$ and matched will with reference PDF card# 73-2340.

In all XRD patterns , the well defined, strong and sharp peaks appeared in the powder profiles of zeolitic products imprinted thier high crystallinity under microwave conditions, meanwhile the absence of any interfering phases indicated the high quality of the crystalline phases.

3.b. SEM and TEM Results

Figure 4a1&2 displays the SEM and TEM micrographs of micro and nano analcime zeolite prepared at 150 °C/4h (M-ANA) and 160 °C/1h (N-ANA) under microwave conditions. The micrograph of the micronized powder (Fig.4a1) implies the characteristic trapezohedral structure of the pseudocubic form of analcime particles with crystal sizes in the range of 15-20 μm . While, the nano species showed rounded crystallites in the size less than 100 nm (Fig.4a2). The micronized sample in Fig.4a1 showed some debris from the parent rock.

Figure 4b1&2 is showing the micrographs of the faujasite-NaX product obtained at the same temperature of 110°C and different durations of 6h and 1h under M-H. The synthetic powders were completely crystallized and the measured crystal sizes were in the range of 1-5 μm (Fig. 4b1) and of about 100 nm (Fig. 4b2) for micro

(M-ZX) and nano faujasite-Na (N-ZX) originated under M-H, respectively.

SEM and TEM micrographs of the final products implied communities of uniformly-sized crystals with narrow particle size distribution and well known crystal configuration for each zeolite type.

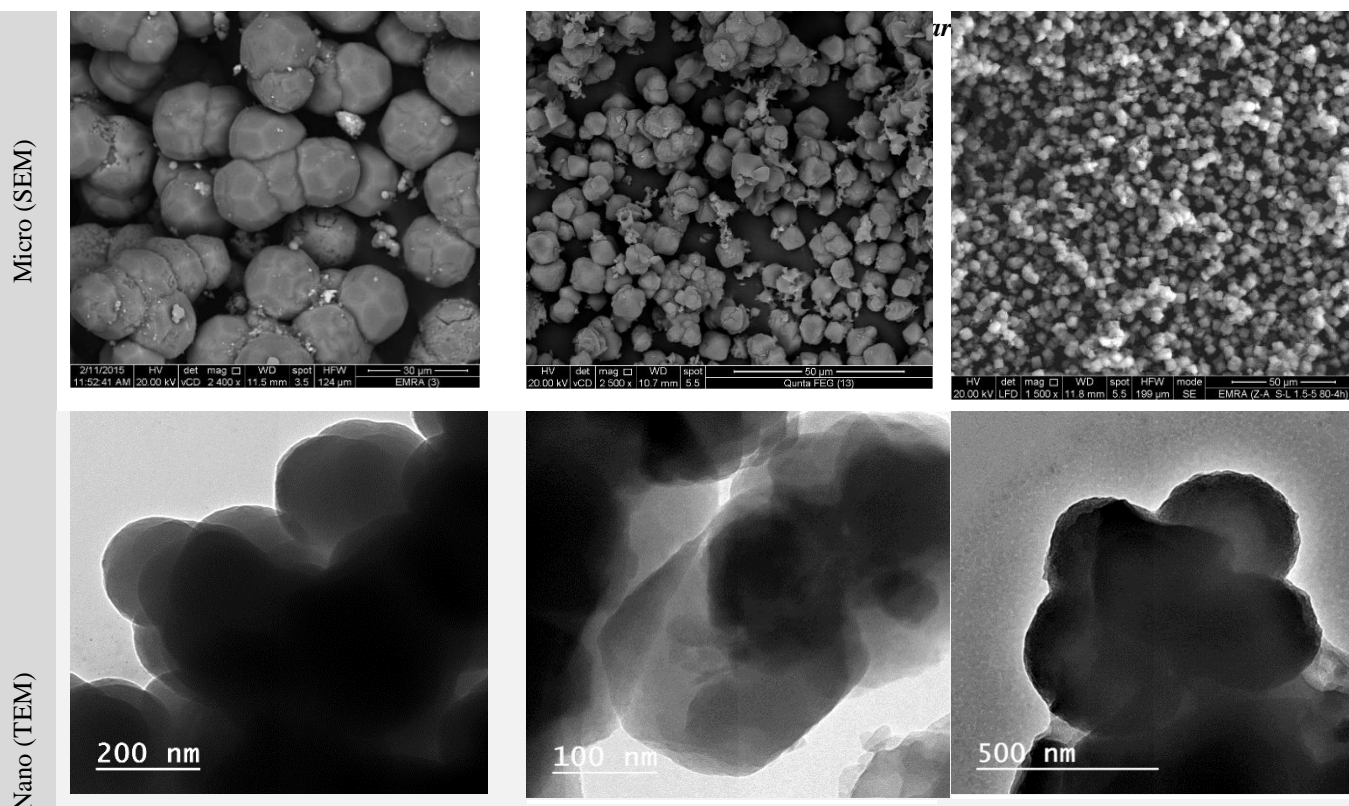


Figure 4a-c) SEM and TEM of the prepared micro and nano- zeolites under different microwave heating.

Figure 4c1&2 configures the SEM and TEM of two zeolite-A samples developed under the same conditions of M-H. The microstructures presented the characteristic cubic morphology of zeolite-A crystals, having N-ZA crystallite size-range of 3-5 μm (Figure 4c1), meanwhile, the N-ZA sample delivered tiny crystals of 100-200 nm in size range (Figure 4c2).

In the previous Figures 1-3, the XRD results showed comparable peak intensities for the micronized and nano-sized zeolites forms. Although, developed at much less time of only 1h, all nano-zeolite XRD profiles seemed properly developed with complete matching to their reference cards. In addition, the solid products were very pure with no interfering phases. In addition,

Figure 5A-C depicts the adsorption/desorption isotherms and the pore size distribution of zeolites with the highest (faujasite-NaX), lowest (analcime), and intermediate BET values. Whereas, calculated specific surface area (BET), total pore volume (TPV) and their corresponding storage capacities (HS) are tabulated in Table 3. In Figure 5, the obtained results showed that, the adsorption-desorption isotherms for tested zeolite species were exhibiting type I isotherm, which is indicative to the microporous nature of zeolite structures, wherein, the desorption is identical to adsorption [44]. It also shows the negligible amount of adsorbed N_2 in

analcime (nano& micro), which is the least in all processed samples (Fig. 5B), compared to the much higher and moderate quantities adsorbed/desorbed into ZX and ZA type, respectively (Fig. 5A).

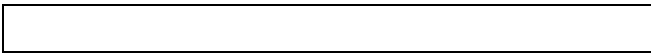


Figure 5; N₂ Adsorption/ desorption isotherms for micro and nano zeolites of A) Faujasite-NaX A, B) Analcime, and C) Zeolite-A.

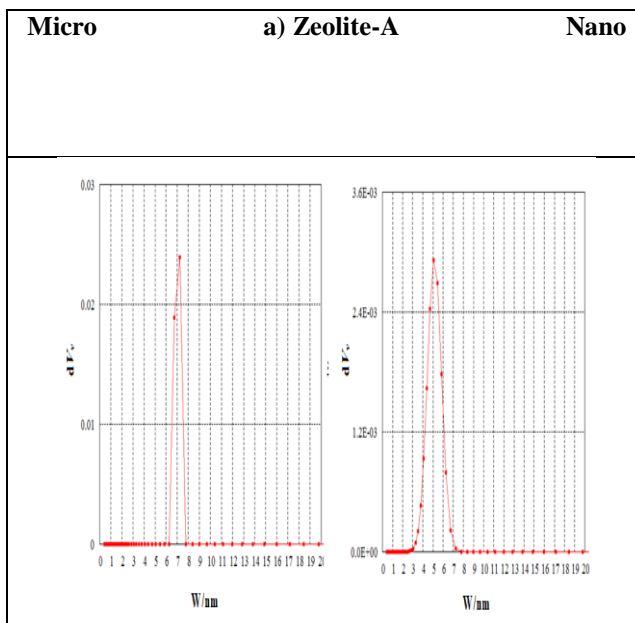
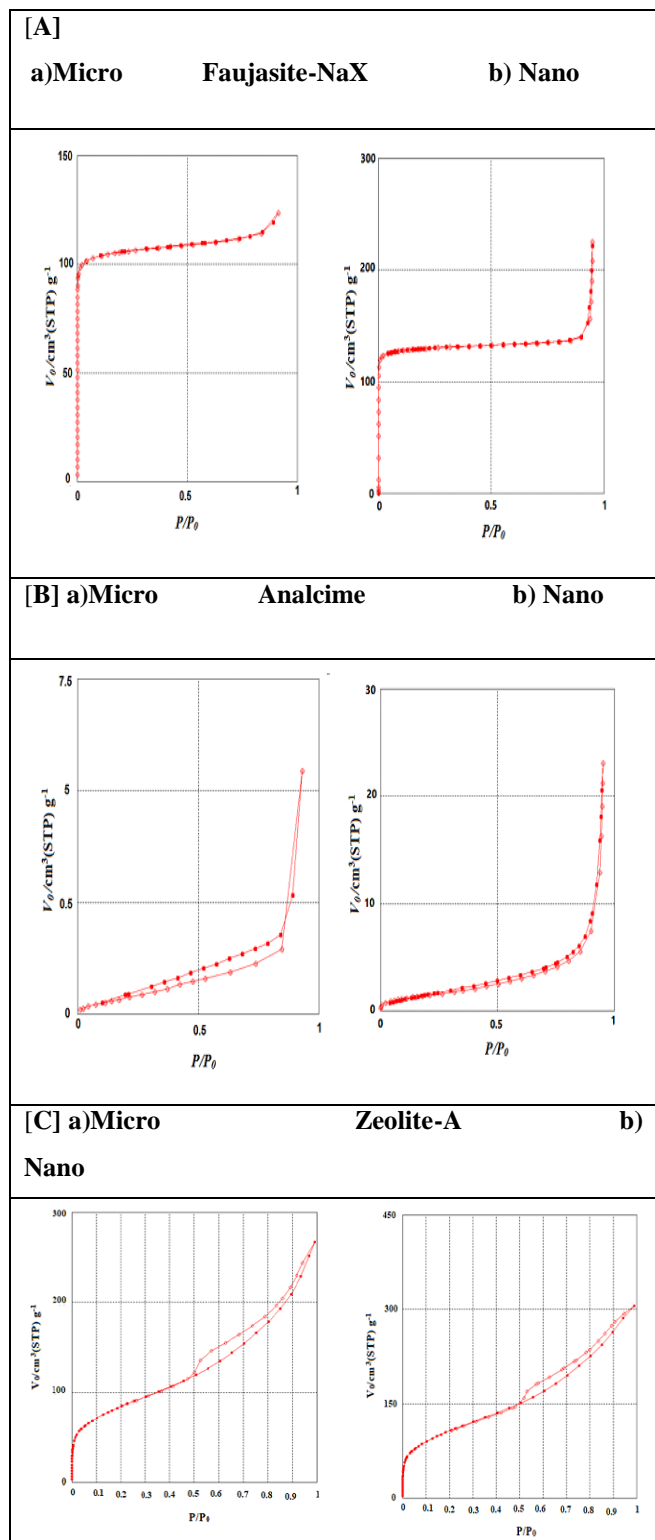
3.d. Hydrogen Storage Results (HS)

Table 3 is showing the textural parameters of different zeolites and their corresponding capacities of hydrogen uptake. Meanwhile, Figure 6a-c presents the pore size distribution of each zeolite framework type.

Table 3: Textural parameters and hydrogen capacities for prepared zeolites.

Zeolite types	Faujasite-NaX (ZX)		Zeolite-A (ZA)		Analcime (ANA)	
	Micro (μm)	Nano (nm)	Micro (μm)	Nano (nm)	Micro (μm)	Nano (nm)
BET(m ² /g)	372	462	276	374	19.2	36
Particle sizes	1-5	100	3-5	100-200	15-20	100
TPV(cm ³ /g)	0.191	0.34	0.082	0.1186	0.0127	0.0178
HS (wt%)	1.67	2.25	1.58	1.94	0.14	0.74

Where; BET: is the surface area, TPV: the total pore volume, and HS: hydrogen storage, μm: micrometer and nm is nanometer.



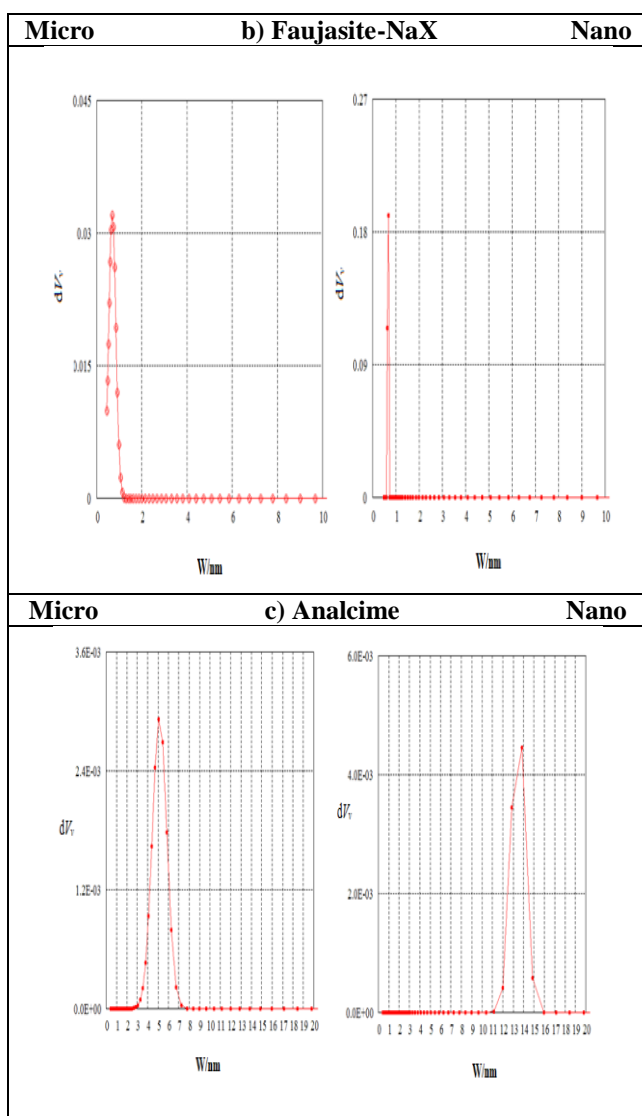
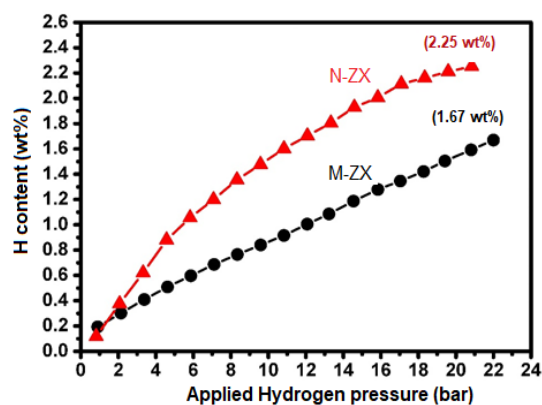


Figure 6a-c: Pore size distribution curves for different zeolites.

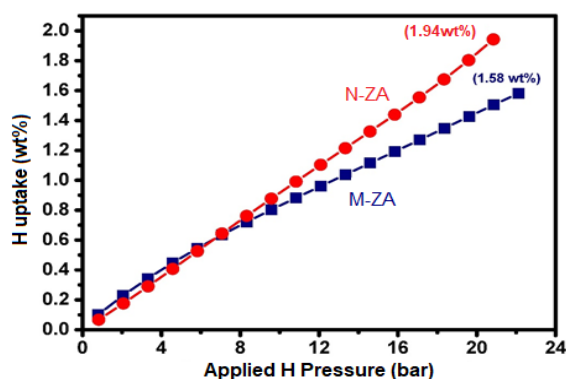
It can be noticed from Table 3 that, the nanoforms of all studied samples measured higher surface area values (BET) than their micronized counterparts. In addition, this BET enlargement is combined with referent increase in the calculated total pore volumes (TPV) with values of descending order of $ZX > ZA >> ANA$. The previous sequential downward trend of both BET and TPV seemed consistent with the zeolite capabilities in hosting hydrogen; ZX has the largest recorded values of both characters which is accompanied with the highest HS capacity, while, ANA and ZA crystals possessed the least and

intermediate values among all measurements, respectively.

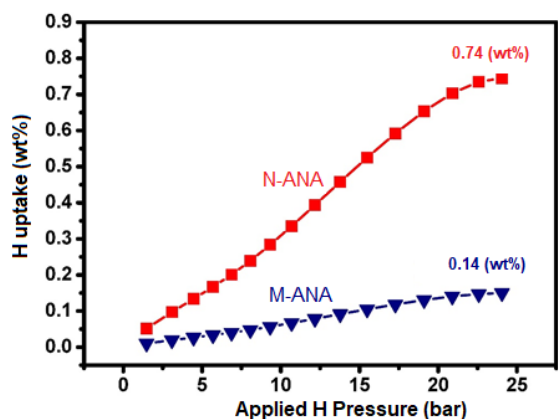
Figure 7a-b shows the Pressure-Composition Isothermal (PCI) configuration of the hydrogen adsorption behaviour for different zeolites under investigation. The storing capacities of the investigated zeolites were measured at 77K and pressure range of 1-22 bar. The maximum amounts of hydrogen stored within the micronized forms of ZX, ZA and ANA zeolites were 1.67, 1.58 and 0.14 wt%, respectively. In comparison, much more hydrogen amounts of 2.25, 1.94 and 0.74 wt% were accommodated in the respective nano species of the same zeolites under the same conditions.



(a)



(B)



(C)

Figure 7a-c: Pressure-Composition Isothermal (PCI) for micro and nano forms of a) Faujasite-NaX (ZX), b) Zeolite-A (ZA), and c) Analclime (ANA).

Based on both the framework structure and pore characteristics, different types of zeolites exhibited remarkably different hydrogen uptake. In a previous work, direct relation was found between the specific surface area of the porous solid and its efficiency in storing hydrogen, which in turn, reflects the number of adsorption sites and the available void volume inside each type [45]. Therefore, the ordinary relation between the BET surface area and volumetric HS capacity is approximately linear [46-47]. Accordingly, and in the present study, the obtained results indicated significant improvement in the volumetric HS capacity on reducing zeolites crystallite sizes, i.e. increasing their BET surface areas (Table 3); the HS ability of ZX raised from 1.67 to 2.25 wt% (Fig. 7a) on minimizing its particle sizes from 5 μm to < 100 nm and enlarging zeolite surface area from 372 to 462 m^2/g . Similarly, micronized zeolite-A (Fig. 7b) showed smaller HS capacity of 1.58 wt%, than its nano powders, which physically adsorbed 1.97 wt% when its surface area increased from 276 to 334 m^2/g , with a corresponding crystallite size reduction from 3-5 μm to <200 nm. Under the same storing conditions, the measured 19.2 m^2/g BET value of the micro-analclime powder was nearly doubled into 36 m^2/g on reducing the particles

from <20 μm (M) to 100 nm (N) in sizes, the net result is a notable multiplication in the HS ability from 0.14 (M) to 0.74 (N) wt% for the micro and nano species, respectively (Fig. 7c).

It is worth mentioning that, the performed reduction in the particle size of zeolite powders, from micro to nano, is reflected in a mutual increase in both total pore volumes (TPV) and measured surface areas (BET). In general, the collected values of TPV and BET for all zeolite entities were comparable, and have a converse relation to the microstructure particle size and direct relation to zeolite hydrogen storage efficiency. (see Table 3). Reasonably, the elevation of HS capacity is the direct expression of the probable amplification of the available void volumes of each species, supplied by its nano texture, and expressed practically as enlarged specific surface area [45-47].

Although, the powders of ZX and ZA have nearly the same size for their micronized (less than 5 μm) and nano (100-200 nm) crystallites, each type indicated different HS capacity. This can simply be explained by the difference in channel dimensions and pore size diameters of each framework structures; Zeolite-A and Faujasite-NaX have channels diameters of 11.2, 6.6, 4.1 & 2.2 \AA , and 13.8, 7.4 and 4.8 \AA , respectively [48-49]. Thus, it is quite expected for the wider micro pores of faujasite (largest pore aperture 7.4 \AA) to promote easier passage and higher capacity for the volumetric storage of physically adsorbed hydrogen than that of smaller one of zeolite-A (with the widest pore diameter of 4.1 \AA).

Irrespective to the improved results obtained from nano-analclime (uptake of 0.74 wt%), compared to its micronized version (0.14 wt%), analclime is truly assigned as the structure with the lowest ability in storing hydrogen among the three tested zeolites. This is quite normal, since it comprises the densest structure assembly (2.25-2.30 g/cm^3) and the narrower pore windows, formed from 8-membered ring framework

with channel dimensions of 0.42x 0.16 nm and the smallest pore openings ever in all zeolites, 0.26 nm [50]. The impact of narrow pores may result in the blocking effects of its channels with a hindering action for hydrogen to diffuse onto the framework vacancies, and locally enabled hydrogen to be adsorbed on the outer surfaces and between grains, with the net resultant of being the least in hosting hydrogen.

In previous literature, it has been shown that, under reduced temperature of 77 K and a pressure of 15 bar, the hydrogen gravimetric capacities were raised from 0.1 wt% at room temperature to a maximum of 2.19 and 1.81 wt% for CaX and NaY, respectively [51-52]. In another report, NaX-type exhibited the largest gravimetric storing capability in zeolites, and stored 2.55 wt% when treated at the same previous temperature and a higher pressure of 40 bar [53]. Accordingly, it has been concluded that, the high hydrogen storing capacity of zeolites is considered as a function of the high pressure and temperature [53]. Compared to the previous literature and in the present work, N-ZX showed more efficient HS ability of 2.25 wt%, under the same previous temperature of 77K, but at nearly much reduced pressure of 22 bar. In the same context, zeolite-A was considered for hydrogen storage at room temperature in another work, the result obtained was 1.2 wt % at 700 bar [31]. A modification of the previous work was carried out on the same species, but with different exchanging cations of Na, Li and K at higher pressures [54]. Authors found that, the uptakes of hydrogen were slightly enhanced to about 0.1 and 0.4 wt% at a pressure of 10 and 60 bar, respectively. Compared to the said references, zeolite-A crystalline powder of this study, implied more ability to store hydrogen with amounts reaching approximately 1.58 wt% for microforms and 1.94 wt% for nano ones at the same temperature of 77 K and much less pressure of only 22 bar.

For the in hand study, the recorded HS capacities for both zeolite-A and faujasite-Na, micro and nano, assigned improved and efficient results for zeolites, as a microporous solid, through tuning of their internal structure into a nano identity. Probably, much tailoring of the microstructures by reducing zeolite crystals to less than 100 μm in sizes, and/ or designing new hollow geometrical forms can help in the surface area enlargement and assist zeolite structures to prospectively host much more hydrogen that can meet the on-board targeted amounts of hydrogen (5.5 wt%), set by US Department of Energy (DOE).

The relative improvement in the volumetric capacity of the prepared zeolites may be attributed to the efficiency of microwave heating in producing solid powders with high crystallinity, uniformly sized particles, of both micro and nano species, with narrow particle-size distribution. This resulted in supplying higher specific surface areas and more exposed internal surfaces to the applied hydrogen pressure and facilitated more hydrogen to penetrate through the material of perfect crystallinity [41,55]. It is well known that, the traditional hydrothermal heating used to deliver microstructures with different spans of crystal sizes and wide particle size distribution range due to the inhomogeneity or localized superheating all over the reaction media [56].

4. Conclusions

In conclusion, three main points can be of practical importance for zeolites to be considered as efficient in storing hydrogen, namely;

1. Production of safe hydrogen storage carriers from natural resource is of economic importance for reasonable energy price.
2. Not only, the enlargement of the surface area is the limiting factor for efficient hydrogen

uptake in zeolites, but also, their microstructures that contain channels with enough pore aperture to enable easier dual passage for hydrogen.

3. Although indicated a slightly higher HS ability on particle size reduction, Analcime zeolite is not practically suitable for hydrogen uptake due to the blocking effect of its channels and the possession of the smallest pore diameter ever in all zeolites, of 0.26nm. Hydrogen molecules were forced to be physically adsorbed on its surfaces rather than diffused into channels.
4. For higher storing capability of zeolite frameworks, more tailoring designs need to be applied with less particle sizes than 100 nm.

5. Acknowledgment

Authors are greatly thankful for the In-house project sector, National Research Centre (NRC), Egypt, for supporting this work.

6. References

- [1] Department of Energy, Target Explanation Document: Onboard Hydrogen Storage for Light-Duty Fuel Cell Vehicles, Department of Energy, 2015. http://energy.gov/sites/prod/files/2015/05/f22/fcto_targets_onboard_hydro_storage_explanation.pdf.
- [2] Multi-Year Research, Development and Demonstration Plan. 2012. <http://energy.gov/sites/prod/files/2014/03/f12/introduction.pdf>.
- [3] Satyapal S., Petrovic J, Read C, Thomas G, and Ordaz G. The U.S. Department of Energy's National Hydrogen Storage Project: progress towards meeting hydrogen-powered vehicle requirements, *Catalysis Today* 2007; 120, 3-4, 246–256.
- [4] Mendoza-Cortes J, Goddard W, Furukawa H, Yaghi O. A covalent organic framework that exceeds the DOE 2015 volumetric target for H₂ uptake at 298 K. *J Phys Chem Lett* 2012; 3,18, 2671–2675.
- [5] Hydrogen posture plan, An Integrated Research, Development and Demonstration Plan, United States Department of Energy, (2006), <http://www.hydrogen.energy.gov>.
- [6] Stolten D. Hydrogen and fuel cells: fundamentals, technologies and applications. *Angewandte Chemie* 2011; 50: 42: 9787.
- [7] Ewald R. Requirements for advanced mobile storage systems. *Inter J Hydrogen Energy* 1998; 23:9:803–814.
- [8] Fichtner M. Nanotechnological aspects in materials for hydrogen storage. *Adv Eng Mater.* 2005; 7: 443-455.
- [9] Langmi H, McGrady G. Non-hydride systems of the main group elements as hydrogen storage materials. *Coord Chem Rev* 2007; 251: 925-9.
- [10] Ismail N, El-Meligi A, Temerk Y, Madian M. Synthesis and characterization of FePS₃ for hydrogen uptake. *Inter J Hydrogen Energy* 2010; 35: 7827 -7834.
- [11] Abdel-Hameed S, Ismail N, Youssef H, Sadek H, Marzouk M. Preparation and Characterization of Mica Glass-Ceramics as Hydrogen Storage Materials. *Inter J Hydrogen Energy* 2017; 42: 6829-6839.

- [12] Wolf G, Baumann J, Baitalow F, Hoffmann F. Calorimetric process monitoring of thermal decomposition of B-N-H compounds. *Thermochim Acta* 2000; 343: 19-25.
- [13] Chaster P, David W, Johnson S, Edwards P, Anderson P. Synthesis and crystal structure of $\text{Li}_4\text{BH}_4(\text{NH}_2)_3$. *Chem. Commun* 2006; 2439-2441.
- [14] Filinchuk Y, Yvon K, Meisner G, Pinkerton F, Balogh M. On the composition and crystal structure of the new quaternary hydride phase $\text{Li}_4\text{BN}_3\text{H}_{10}$. *Inorg. Chem* 2006; 45: 1433-1435.
- [15] Menon VC, Komarneni S. Porous adsorbents for vehicular natural gas storage: a review. *J Porous Mater* 1998; 5:43-58.
- [16] Carpetis C, Peschka W. A study on hydrogen storage by use of cryoadsorbents. *Int J Hydrogen Energy* 1980; 5: 539-554.
- [17] Agarwal P, Noh J, Schwarz J, Davini P. Effect of surface acidity of activated carbon on hydrogen storage. *Carbon* 1987; 25: 2: 219-226.
- [18] Chahine R, Bose T. Low-pressure adsorption storage of hydrogen. *Int. J Hydrogen Energy* 1994; 19: 2:161-164.
- [19] Prabhukhot Prachi R., Wagh Mahesh M., Gangal Aneesh C. A Review on solid state hydrogen storage materials, *Adv Energy Power* 2016; 4:2: 11-22.
- [20] Catlow C. Zeolites: Structure, Synthesis and Properties – An Introduction. In: *Modeling of Structure and Reactivity in Zeolites*, Ed. Catlow, Academic Press, UK 1992.
- [21] Ernst S, Fritz M, Weitkamp J. Zeolites as Media for Hydrogen Storage. *Int. J. Hydrogen Energy* 1995; 20:12: 967-970.
- [22] Hurlbut C, Cornelius S, Cornelis K, 1985, *Manual of Mineralogy*, 20th ed. Wiley 1993; ISBN 0-471:80580-7. Klein, C. and Hurlbut, CS 1993.
- [23] Teertstra D, Černý P. Controls on morphology of analcime-pollucite in natural minerals, synthetic phases, and nuclear waste products. *Cryst Res Technol* 1992; 27: 931-939.
- [24] Putnis A, Giampaolo A, Graeme-Barber A (1993). High temperature X-ray diffraction and thermogravimetric analysis of the dehydration of analcime, $\text{NaAlSi}_2\text{O}_6 \cdot \text{H}_2\text{O}$ EUG VII, Strasbourg, France, *Terra Abstracts* 1993: 5: 497.
- [25] Hriljac J, Eddy M, Cheetham A, Donohue J, Ray G. Powder Neutron Diffraction and ^{29}Si MAS NMR Studies of Siliceous Zeolite-Y. *J Solid St Chem.*1993; 106: 66-72.
- [26] Bekkum V, Jansen J, Flanigen E. *Introduction to Zeolite Science and Practice* 1991; 58: 13-33.
- [27] Basmadjian D. Adsorption equilibria for hydrogen, deuterium and their mixtures. Part 1. *Canad. C.Chem.* 1960; 38:141-148.
- [28] Skazvaev VE, Khovshchev SS, Zhdanove SP. Low-temperature adsorption of hydrogen on synthetic zeolites. *Russ. Chem. Bull.* 1975; 24: 1143-1147.
- [29] Levin MA, Gorbuno MB, Moskovskaya TA, Sperinskii VV, Yakubov TS. Adsorption of hydrogen isotopes at high pressure. *Russ. Chem. Bull.* 1986;35: 2406-2408.
- [30] Kazansky VB, Borovkov VY, Serich A, Karge HG. Low temperature hydrogen adsorption on sodium forms of faujasites: Barometric measurements and drift spectra. *Microp. Mesop. Mater.* 1998;22: 251-259.
- [31] Langmi HW, Book D, Walton A, Johnson SR, Al-Mamouri MM, Speight JD, Edwards PP, Harris IR, Anderson PA. Hydrogen storage in non-exchanged zeolites. *J. Alloy Comp.* 2005; 404-406: 637-642.
- [32] Li YW, Yang RT. Hydrogen storage in low silica type X zeolites, *J. Phys. Chem. B* 2006; 110: 17175-17181.
- [33] Nikolas M. Musyoka, Jianwei Ren, Henrietta W. Langmi, Brian C. North, Mkhulu Mathe. A comparison of hydrogen storage capacity of commercial and fly ash-derived zeolite X together with their respective template carbon derivative, *Int. J. Hydrogen Storage Energy* 2015; 40: 12705-12712.
- [34] Vitillo J, Ricchiardi G, Spoto G, Zecchina A. Theoretical maximal storage of hydrogen in

- zeolite frameworks. *Phys. Chem. Chem. Phys.* 2005; 7:3948-3954.
- [35] Felderhoff M, Weidenthaler C, von Helmolt R, Eberle U. Hydrogen storage: the remaining scientific and technological challenges. *Phys Chem Phys* 2007; 9: 2643–2653.
- [36] Breck D. Zeolite Molecular sieves- Structure, Chemistry and uses. John Wiley, New York, 1974.
- [37] Panella B, Hirscher M. Hydrogen physisorption in metal–organic porous crystals. *Adv Mat* 2005; 17: 538-541.
- [38] Barbara B, Hirscher M, Putter H, Muller U. Hydrogen Adsorption in Metal–Organic Frameworks: Cu-MOFs and Zn-MOFs Compared. *Adv Funct Mat* 2006; 16:4: 520-524.
- [39] Broom D, Webb C, Hurst K et al. Outlook and challenges for hydrogen storage in nanoporous materials. *Appl. Phys. A* 2016; 122:151. doi:10.1007/s00339-016-9651-4
- [40] Youssef H, Ibrahim D, Komarneni S. Microwave-Assisted versus Conventional Hydrothermal Synthesis of Zeolite A from Metakaolinite. *Micro Meso Mat* 2008; 115: 527-534.
- [41] Youssef H.F, Hanan Abo-almaged; Wael Hegazy; Gehan El-Bassyouni. Novel synthesis method of micronized Ti-Zeolite Na-A and cytotoxic activity of its silver exchanged form. *Bioinorganic Chemistry and Applications*, Volume 2015, Article ID 428121, 12 pages. Hindawi Publishing Corporation.
- [42] Youssef H.F, Abdel-Aziz M.S, Fouda F. K. Evaluation of Antimicrobial Activity of Different Silver-exchanged Nano and Micronized Zeolites prepared by Microwave technique. *J. Porous Materials*, 24, pp 947-957.
- [43] Sing K, Everett D, Haul R, Moscou L, Pierott R, et al. Reporting physisorption data for gas/solid systems with special reference to the determination of surface area and porosity (Recommendations 1984). *Pure Appl Chem* 1985; 57: 603-19
- [44] Rameirez-Cuesta A, Mitchell P, Ross D, Georgiev P, Anderson P, et al. Dihydrogen in cation-substituted zeolites X-an inelastic neutron scattering study. *J Mater Chem* 2007; 17: 2533-2539.
- [45] Hirscher M. Hydrogen Storage by Cryoadsorption in Ultrahigh-Porosity Metal–Organic Frameworks. *Angewandte Chemie Inter Edition* 2011; 50:3: 581-582.
- [46] Hirscher M, Panella B, Schmitz B. Metal-organic frameworks for hydrogen storage. *Microporous mesoporous mat* 2010; 129:3:335-339.
- [47] Kuronen M, Harjula R, Jernstrom J, Vestenius M, Lehto J. Effect of the framework charge density on zeolite ion exchange selectivities. *Phys. Chem. Chem. Phys.* 2000; 2: 2655–2659.
- [48] Kabwadza-Corner P.; Munthali, M, Johan E, Matsue N. Comparative study of copper absorptivity and selectivity toward zeolites. *Am J Anal Chem* 2014; 5: 395–405.
- [49] Mumpton F. La roca magica: uses of natural zeolites in agriculture and industry. *Proc. Natl. Acad. Sci. USA* 1999; 96:3463–3470.
- [50] Harris I, Walton A, AL-Mamouri M, Johnson S, Book D, et al. Hydrogen storage in ion-exchanged zeolites. *J Alloys Comp.* 2005; 404-406: pp. 637-642.
- [51] Langmi H, Walton A, AL-Mamouri M, Johnson S, Book D, et al. Hydrogen adsorption in zeolites A, X, Y and RHO. *J Alloys Comp* 2003; 3560357:710-715.
- [52] Xiao-ming Du, Er-Dong Wu. Physisorption of hydrogen in A, X and ZSM-types of zeolites at moderately high pressures. *Chin. J. Chem. Phys* 2006; 19: 457-463.
- [53] Darkrim F, Aoufi A, Malbrunot P. Hydrogen adsorption in the NaA zeolite: a comparison between numerical simulations and experiments. *J Chem Phys* 2000; 112: 13: 5991-5999.
- [54] Kayiran S, Darkrim. Synthesis and ionic exchanges of zeolites for gas adsorption. *Surf Interface Anal* 2002; 34: 100-104.
- [55] Sathupunya M, Gulari E, Jamieson A, Wongkasemjit S. Microwave-assisted preparation of zeolite K-H from alumatrane and

silatrane. *Microporous Mesoporous Mater* 2004; 69:3: 157–164.

- [56] Newalkar B, Olanrewaju J, Komarneni K, Microwave- hydrothermal synthesis and characterization of Zirconium substituted SBA-15 mesoporous silica, *J Phys Chem* 2001; 105: 8356-8360.